We are IntechOpen, the world's leading publisher of Open Access books Built by scientists, for scientists

4,800
Open access books available

122,000
International authors and editors

135M
Downloads

Our authors are among the

154
Countries delivered to

TOP 1%
most cited scientists

12.2%
Contributors from top 500 universities

CLARIVATE ANALYTICS BOOK CITATION INDEX INDEXED

WEB OF SCIENCE™

Selection of our books indexed in the Book Citation Index in Web of Science™ Core Collection (BKCI)

Interested in publishing with us?
Contact book.department@intechopen.com

Numbers displayed above are based on latest data collected.
For more information visit www.intechopen.com

6

Acoustic Waves: A Probe for the Elastic Properties of Films

Marco G. Beghi
Politecnico di Milano, Energy Department and NEMAS Center, Milano Italy

1. Introduction

Films and thin films are exploited by an ever increasing number of technologies. The properties of films can be different from those of the same material in bulk form, and can depend on the preparation process, and on thickness. Specific techniques are needed for their measurement. Whenever films or thin layers have structural functions, as in micro electro-mechanical systems (MEMS), a precise characterization of their stiffness is crucial for the design of devices. The same can be said for the design of devices which exploit thin layers to support surface acoustic waves (surface acoustic wave filters). More generally, knowledge of the elastic properties is interesting because such properties depend on the structural properties.

The most widespread technique for the mechanical characterization of films, instrumented indentation, induces both elastic and inelastic strains. It also characterizes irreversible deformation, but the extraction of the information concerning the elastic behaviour is non trivial. To overcome this difficulty, several measurement methods have been developed, which exploit vibrations as a probe of the material behaviour. These methods intrinsically involve only elastic strains, and are non destructive. This is true at any length scale, and is peculiarly useful at micrometric and sub-micrometric scales, where the exploitation of other types of probes can become critical.

Both propagating waves and standing waves can be exploited, with excitation which can be either monochromatic (e.g. resonance techniques) or impulsive, therefore broadband, requiring an analysis of the response either in the time domain (the so called picoseconds ultrasonics) or in the frequency domain (the so called laser ultrasonics). The propagation velocities of vibrational modes are obtained, from which the stiffness is derived if an independent value of the mass density (the inertia) is available.

Older resonance techniques have been developed to be operated with thin slabs, also exploiting optical measurements of displacement. In the measurement of films and small structures, the advantages of light, a contact-less and inertia-less probe, are substantial, and are increasingly exploited. The laser ultrasonics technique, commercially available since some years ago, measures waves travelling along the film surface. The so called picosecond ultrasonics technique measures waves travelling across the film thickness; it is a relatively sophisticated optical technique, which exploits femtosecond laser pulses in a pump-and-probe measurement scheme. For best performance it needs the deposition of

an interaction layer, possibly combined with microlithography techniques to obtain a patterned layer.

Techniques for optical detection of acoustic vibrations include inelastic scattering of light: Brillouin scattering. Brillouin spectroscopy does not excite vibrations, but relies on thermal excitation, which has the broadest band but small amplitude, and measures the spectrum of inelastically scattered laser light. Brillouin Spectroscopy and Surface Brillouin Spectroscopy are relatively simple optical techniques, which do not require a specific specimen preparation. They operate at sub-micrometric acoustic wavelengths, which are selected by the scattering geometry, and have been exploited to characterize the elastic properties of bulk materials and of films.

An overview of this variety of techniques is presented here, underlining analogies and differences. The increasing demand of precise characterization raised the point of precision and accuracy achievable by vibration based techniques, and specifically by the optical techniques. In the overview, attention is drawn to the steps or the parameters which are the limiting factor for the achievable precision, and to the way of characterizing them. The effects of inaccuracies of the mass density are common to all the techniques based on vibrations, while other sources of uncertainty are more specific to each technique.

2. Acoustic modes in elastic solids

In the continuum description the instantaneous configuration of a solid undergoing deformation can be represented by the displacement vector field $\mathbf{u}(\mathbf{r},t)$, where $\mathbf{u}=(u_1,u_2,u_3)$, $\mathbf{r}=(x_1,x_2,x_3)$ and t is time. The local state of the solid being represented by the strain and stress tensors, the linear elastic behaviour is characterized by the tensor of the elastic constants C_{ijmn}, which can be conveniently represented by the matrix of the elastic constants C_{ij}. When other phenomena, like e.g. viscoelasticity or elasticity of higher orders, can be neglected, the tensor of the elastic constants fully characterizes the stiffness. Inertia is characterized by the mass density ρ. Within a homogeneous linear elastic solid, in the absence of body forces, the equations of motion for the displacement vector field are homogeneous, and read (Auld, 1990; Every, 2001; Kundu, 2004)

$$\rho\frac{\partial^2 u_i}{\partial t^2}=\sum_{j,m,n}C_{ijmn}\frac{\partial^2 u_m}{\partial x_j\partial x_n},\quad i=1,2,3\quad . \tag{1}$$

These equations describe vibrational elastic excitations, which are typically called acoustic also in the ultrasonic frequency range. The basic solutions of Eqs.(1), and the most important ones when boundary effects are irrelevant, are the plane acoustic waves, or modes (Auld, 1990; Kundu, 2004), of the form

$$\mathbf{u}=\mathbf{e}\Re\left\{\tilde{A}\exp\left[i\left(\mathbf{k}\cdot\mathbf{r}-\omega t\right)\right]\right\}\quad , \tag{2}$$

where $\mathbf{k}$ is the wavevector, $\omega = 2\pi f$ the circular frequency, f the frequency, $\tilde{A}$ an arbitrary complex amplitude, and $\mathbf{e}$ the polarization vector, which is normalized. The continuum description, underlying Eq. (1), is appropriate until the wavelength $\lambda=2\pi/|\mathbf{k}|$ is much larger than the interatomic distances. The three translational degrees of freedom of each infinitesimal volume element correspond, for each wavevector $\mathbf{k}$, to three independent

modes, having different polarization vectors and frequencies. In general the phase velocity $v = \omega / |\mathbf{k}| = \lambda f$ depends on both the direction of **k** and the polarization vector **e**. In an infinite homogeneous medium, travelling waves of the type given by Eq. (2) exist for any frequency *f* compatible with the mentioned lower limit for wavelength.

In the simplest case, the isotropic solid, the matrix of the elastic constants is fully determined by only two independent quantities; the only non null matrix elements are $C_{11} = C_{22} = C_{33}$, $C_{44} = C_{55} = C_{66}$, $C_{12} = C_{13} = C_{23} = C_{11} - 2C_{44}$. In this case the shear modulus *G* coincides with C_{44}, while Young modulus *E*, Poisson's ratio ν and bulk modulus *B* are respectively given by (Every, 2001; Kundu, 2004)

$$E = \frac{C_{44}\left(3C_{12} + 2C_{44}\right)}{C_{12} + C_{44}} = \frac{C_{44}\left(3C_{11} - 4C_{44}\right)}{C_{11} - C_{44}}, \tag{3}$$

$$\nu = \frac{C_{12}}{C_{11} + C_{12}} = \frac{C_{11} - 2C_{44}}{2\left(C_{11} - C_{44}\right)} = \frac{E}{2G} - 1, \tag{4}$$

$$B = \frac{C_{11} + 2C_{12}}{3} = C_{11} - \frac{4}{3}C_{44}, \tag{5}$$

In the isotropic case the phase velocities are independent from the direction of **k**, only depending on the relative orientation of **e** with respect to **k**; one of the three modes is longitudinal ($\mathbf{e} \| \mathbf{k}$) and has velocity v_l, the other two are transversal ($\mathbf{e} \perp \mathbf{k}$), are independent (the two polarization vectors are orthogonal) and degenerate: they have the same velocity v_t (Auld, 1990; Kundu, 2004). The two velocities are

$$v_l = \sqrt{C_{11} / \rho} \quad \text{and} \quad v_t = \sqrt{C_{44} / \rho} \ . \tag{6}$$

In the non isotropic case more than two independent quantities are needed to determine the matrix of the elastic constants, and the phase velocities, beside depending on the direction of **k**, have a more complex dependence on the C_{ij} values.

In a finite geometry the search for standing waves having the harmonic time dependence of the type $e^{-i\omega t}$ transforms Eq. (1) into an eigenfunction / eigenvalue equation of the Helmholtz type (Auld, 1990); an appropriate set of basis functions allows to transform this equation into a matrix eigenvalue problem (Nakamura et al., 2004). The eigenvalues are proportional to ω^2, the square of the frequencies of the acoustic modes of the structure, or natural frequencies of the structure. In other words, the finiteness of the geometry converts the continuum spectrum of frequencies of the modes of the infinite medium, given by Eq. (2), into the discrete spectrum of the natural frequencies. These frequencies depend on the (C_{ij}/ρ) values and on the geometry.

In a schematic way: also in non isotropic media the acoustic velocities depend on stiffness and inertia as in Eqs. (6): $v^2 = C / \rho$, indicating generically by *C* the relevant combination of elastic constants and, possibly, direction cosines of **k**. In the simplest case, the one dimensional geometry of length *L*, the standing waves are identified by the constructive self interference condition $L = n\lambda / 2 = (n/2)v / f$ (n is an integer number), such that $f = (n/2)\sqrt{C/\rho} / L$. Therefore, a measurement of the frequencies of the acoustic modes

allows to derive $C = \rho(fL)^2 / (n/2)^2$. Also in more complex geometries, the dependence is of the same type

$$C = \rho(fL)^2 N \tag{7}$$

where L is now a characteristic length of the structure (for a slender rod, essentially one dimensional, the length), and N is a dimensionless numerical factor which, beside the mode order n, can depend on dimensionless quantities like geometrical aspect ratios or Poisson's ratio. The factor N also depends on the character of the mode whose frequency f is being measured, and therefore on the specific modulus C which is involved.

Structures can be finite in one or two dimensions and practically infinite in others, as it happens e.g. in a slab or a long cylinder. The free surface of an otherwise homogeneous solid is a case of semi-infiniteness along a single dimension. The translational symmetry is broken in the direction perpendicular to the surface, and new phenomena, absent in the infinite medium, are found: the reflection of bulk waves, and the existence of surface acoustic waves. Namely, at a stress free surface Eqs. (1) admit a further solution: the Rayleigh wave, the paradigm of the surface acoustic waves (SAWs). Such waves have peculiar characters (Farnell & Adler, 1972): a displacement field confined in the neighborhood of the surface, with the amplitude which declines with depth, a wavevector parallel to the surface, and a velocity lower than that of any bulk wave, such that the surface wave cannot couple to bulk waves, and does not lose its energy irradiating it towards the bulk. Pseudo surface acoustic waves can also exist, which violate this last condition. The velocity v_R of the Rayleigh wave cannot be given in closed form; in the isotropic case a good approximation is (Farnell & Adler, 1972)

$$v_R \cong v_t \frac{0.862 + 1.14\nu}{1+\nu} \quad . \tag{8}$$

The continuum model of a homogeneous solid does not contain any intrinsic length scale. Accordingly, all the solutions for this model are non dispersive, meaning that the velocities (Eqs. (6) and (8)) are independent from wavelength (or frequency).

More complex modes occur in non homogeneous media. Layered media are a particularly relevant case, in which new types of acoustic modes can occur; namely, modes confined around the interfaces and modes which are essentially guided by one layer or another, like the Sezawa waves. In this case, also in the continuum model the physical system has an intrinsic length scale, identified by the layer thicknesses. For wavelengths much smaller than the thicknesses wave propagation occurs within each layer as if it was infinite, with reflections and refractions at the surfaces. Instead, for wavelengths comparable to, or larger than, the thicknesses, the acoustic modes extend over several layers, and are modes of the whole structure. Such modes are dispersive: their velocities depend on wavelength, or, more precisely, on the wavelength to thickness ratio(s). Also the simplest surface wave, the Rayleigh wave of a bare homogeneous substrate, is modified by a layer deposited on it, and becomes dispersive: the propagation velocity depends on wavelength, therefore on frequency. The velocities of the acoustic modes in layered structures can be numerically computed, as non trivial functions of the properties of the substrate and the layer(s), and of the wavelength to thickness ratio. The dispersion relations $\omega(k)$ or $v(f)$ are thus obtained.

3. Stiffness measurements

3.1 Vibration based methods

It has always been recognized that since the phase velocities of acoustic waves and the natural frequencies of the acoustic modes depend on stiffness and inertia, their measurement gives access, by Eq.(6) or Eq. (7), to the elastic constants C_{ij}, if the mass density ρ, and possibly the geometry, are known. Many experimental methods have been devised, which exploit vibrations to measure the elastic properties of solids. These methods measure the dynamic, or adiabatic, elastic moduli; these moduli do not coincide with the isothermal moduli which are measured in monotonic tests (if strain rate is not too high), but in elastic solids the difference between adiabatic and isothermal moduli seldom exceeds 1% (Every, 2001). Furthermore, when the elastic constants are needed to design a device which operates dynamically, like most microdevices, the dynamic moduli are exactly the ones which are needed in the design process.

Some methods measure the wave propagation velocity by measuring the transit time over a finite, macroscopic distance, other methods measure the frequency of standing modes defined by the sample geometry, or the frequency of propagating waves of well defined wavelength. The excitation can be either monochromatic, at a frequency which typically should be adjustable until resonance conditions are achieved, or broadband. The latter is typically obtained by an impulsive excitation, which can be provided by a mechanical percussion or by a laser pulse. Generally, the response to a broadband excitation is spectrally analyzed. The availability of ultrafast lasers (femtosecond laser pulses) also allows an analysis in the time domain, by pump-and-probe techniques.

In homogeneous specimens each propagation velocity, or the frequency of each standing wave, has a single value, from which the corresponding elastic modulus can be derived. In non homogeneous specimens, typically in supported films, each propagation velocity can depend on wavelength or frequency. Dispersion relations $\omega(k)$ or $v(\lambda)$ can be measured over a finite interval of frequency or wavelength, and the film properties can be obtained fitting the computed dispersion relations to the measured ones.

3.2 Vibration excitation and detection techniques

The various experimental methods operate in different frequency ranges. The range is determined by both the excitation and the detection techniques, and is strictly correlated to the spatial resolution. It is worth remembering that the acoustic velocities in typical elastic solids like metals and ceramics are of the order of a few km/s = mm×MHz, and that a phase velocity v links the frequency f to a characteristic length L, which can be a characteristic dimension of a structure supporting standing waves, or the wavelength of a travelling wave.

Characteristic lengths of centimetres imply frequencies in the tens of kHz range, which are easily excited by a mechanical percussion and measured by a microphone; Nieves et al. (2000) estimate at around 0.1 MHz the upper limit of the frequencies excited by the mechanical percussion, with a steel ball of a very few millimetres. Piezoelectric actuators, and sensors are also available.

Characteristic lengths of several micrometers correspond to frequencies in the tens of MHz range. Structures of this size can be built by micromachining techniques, and their vibration can be excited and detected by capacitive actuators and sensors. Measurement techniques of this type are essentially a miniaturization of the vibrating reed technique (Kubisztal, 2008). Czaplewski et al. (2005) built flexural and torsional resonators of tetrahedral amorphous

carbon (also known as amorphous diamond), by standard techniques for the production of micro-electromechanical systems. They exploited piezo-electric actuation, and an interferometric technique to measure the oscillation. They were able to perform measurements at variable temperatures, determining the elastic moduli of this material as function of temperature. They analyzed the uncertainty sources, finding that the leading contribution to the uncertainty comes, for the flexural oscillator, from the value of the mass density of this material, while for the torsional oscillator it comes from the exact dimensions of the thin member undergoing torsion.

In larger structures, waves at frequencies in the tens of MHz range can be excited and detected by piezoelectric elements, possibly operating simultaneously as actuators and sensors. Excitation can also be performed by a laser pulse; if the pulse is short enough, the upper limit of the measurable frequency range can be set by the piezoelectric sensor. Optical detection techniques are also available. Specific devices like interdigitated transducers (IDTs) can be built by lithographic techniques on, or within, an appropriate layer stack, which must include a piezoelectric layer. Such devices emit and receive waves at the wavelength which resonates with the periodicity of the transducer, typically at micrometric scale. This configuration was exploited to measure the material properties (Bi et al. 2002; Kim et al., 2000), but it is seldom adopted, because it requires the production of a dedicated micro device.

Micrometric and sub-micrometric wavelengths correspond to frequencies in the GHz to tens of GHz range. Detection of such frequencies requires optical techniques; excitation of such frequencies can be obtained by laser pulses of short enough duration.

The variety of vibration based methods to measure the stiffness of solids the can be classified according to various criteria. In this chapter methods are reviewed grouping them by the main vibration excitation techniques: mechanical excitation, either periodic or by percussion, laser pulse excitation, and inelastic light scattering (Brillouin spectroscopy). Similarly to Raman spectroscopy, Brillouin spectroscopy does not excite vibrations at all, but relies on the naturally occurring thermal motion. This gives access to the broadest band, but with small vibration amplitudes, which require time consuming measurements.

3.3 Precision and accuracy

In all the techniques based on vibrations the elastic constants themselves are not the direct outcome of the measurement, but are derived from direct measurements of a primary quantity like frequency or velocity, and 'auxiliary' quantities like thickness, or mass density. The uncertainty to be associated to the resulting value of each elastic constant must be evaluated considering the uncertainties associated to each of the raw measurements. For a quantity q which is derived from directly measured quantities a, b and c, the uncertainty σ_q depends on the 'primary' uncertainties σ_a, σ_b and σ_c. For a functional dependence of the type $f = Aa^{\alpha}b^{\beta}c^{\gamma}$, where A is a numerical constant, the usual error propagation formula can be written in terms of the relative uncertainties (σ_a / a), (σ_b / b), (σ_c / c) as

$$\left(\frac{\sigma_q}{q}\right)^2 = \alpha^2\left(\frac{\sigma_a}{a}\right)^2 + \beta^2\left(\frac{\sigma_b}{b}\right)^2 + \gamma^2\left(\frac{\sigma_c}{c}\right)^2 \tag{8}$$

However, the various uncertainties can have different meanings and consequences. The frequency is typically measured either identifying the frequency of a periodic signal which achieves resonance, or by the spectral analysis of the response to a broadband excitation. In

both cases each frequency reading is associated to a finite degree of uncertainty, mainly due to random errors. In a set of repeated measurements such errors are uncorrelated, and tend to be cancelled by an averaging process; the error of each measurement affects the dispersion of results around the average, but not the average itself. In other words, these errors affect precision, but not accuracy. The accuracy of results is at most affected by the finite accuracy in the calibration of the frequency meter, of whichever nature it be. When then deriving the elastic moduli, the frequency reading can be exploited as such (see e.g. Eq.(7)), or via the determination of a propagation velocity. In both cases, the obtained moduli also depend on further 'auxiliary' parameters. In a very simple case, from Eq. (6) we have $C_{11} = \rho v_l^2$, and the resulting value of C_{11} is also affected by the finite uncertainty of the best available value of ρ, exploited in the derivation. However, in a set of repeated measurements the uncertainty of ρ does not contribute to the dispersion of results around the average, but it affects the average itself. This means that it affects accuracy, but not precision. The same can be said for the sample geometry (see Eq. (7)).

4. Mechanical excitation

Mechanical excitation can be either impulsive and broadband, as obtained by a percussion, or narrow band, as provided by a periodic excitation. Most methods exploiting mechanical excitation rely on the identification of the natural frequencies, or resonances, of a structure. With a periodic excitation, such frequencies are identified scanning the excitation frequency until resonance conditions (maximum oscillation amplitude for given excitation force) are detected. With a broadband excitation the response (measured amplitude) is frequency analyzed to identify the resonant frequencies.

Among the methods adopting harmonic excitation, acoustic microscopy (Zinin, 2001) exploits a piezoelectric actuator, typically in the form of an acoustic lens, and often operating also as a transducer. The acoustic lens is mechanically coupled to the sample by a liquid drop. Acoustic microscopy can be operated with imaging purposes; in the quantitative acoustic microscopy version (Zinin, 2001) it aims at measuring the acoustic properties of the sample.

Beside acoustic microscopy, two main types of methods have been developed. The first one measures the bulk properties. It adopts macroscopic homogeneous samples, and can exploit either broadband or narrow band excitation. These methods have also been ruled by norms (ASTM, 2008, 2009). A second group of methods, collectively called Resonance Ultrasound Spectroscopy, aims at measuring the properties of thin supported films. It almost invariably exploits a periodic excitation, whose frequency is swept in order to achieve resonance conditions.

4.1 Measurement of bulk properties

Macroscopic homogeneous samples are self supporting. They can be tested as free standing samples, provided the disturbances to free oscillations are minimized. Such a minimization includes sample suspension by thin threads, or specimen support by adequate material (cork, rubber), the supports having contact of minimum size, and positions at the nodes of the fundamental vibrational mode of interest, either flexural or torsional. Also the sensor contact, if oscillation is detected by a contact device, must be devised aiming at the minimization of the disturbance induced by the contact. Non contact detection techniques

are available, including all optical techniques, and acoustic techniques: in the proper frequency range, oscillations can be detected through the air, by a microphone, and even excited, with harmonic excitation, by a similar technique, exploiting an audio oscillator and an audio amplifier. The optical techniques, intrinsically contact-less and inertia-less, have the broadest band, only limited by the light detection and analysis apparatus.

Since the full characterization of the elasticity of an isotropic medium requires two independent parameters, it typically requires excitation of at least two modes of different nature. For a specific simple geometry, the slender rod of length L, test methods have been regulated by norms (American Society for Testing and Materials [ASTM], 2008, 2009, and other ASTM norms cited by these two). Mainly flexural and torsional modes are considered, for a slender rod of mass m, and either rectangular section of width b and thickness t, or circular section of diameter D. Mass density being measured as $\rho = m/(tbL)$, Eq.(7) takes in this case, for the rectangular section, the forms (ASTM, 2008)

$$E = \left[m/(tbL) \right] \left(f_f L \right)^2 \times 0.9465 (L/t)^2 T_E (\nu, L/t) \tag{9a}$$

$$G = \left[m/(tbL) \right] \left(f_t L \right)^2 \times 4 T_G (b/t, b/L) \tag{9b}$$

where f_f and f_t are the frequencies of respectively the fundamental flexural and torsional modes, and T_E and T_G are numerical factors, functions of the indicated dimensionless quantities. Similar formulas hold for rods of circular section. The fundamental frequencies can be identified by either sweeping the frequency of a periodic excitation (ASTM, 2008), or by the broadband excitation by a mechanical percussion (ASTM, 2009), followed by the frequency analysis of the response. In both cases the displacement can be sensed by a contact transducer or by a microphone. The estimates for E and G being coupled by the value of Poisson's ratio (Eqs. 4 and 9a), an iterative procedure is indicated, to obtain consistent estimates. The algorithm of Eq.(8) applied to Eq. (9a) gives

$$\left(\frac{\sigma_E}{E} \right)^2 = \left(\frac{\sigma_m}{m} \right)^2 + 3^2 \left(\frac{\sigma_t}{t} \right)^2 + \left(\frac{\sigma_b}{b} \right)^2 + 3^2 \left(\frac{\sigma_L}{L} \right)^2 + 2^2 \left(\frac{\sigma_f}{f} \right) \tag{10}$$

similar expressions being obtained for (σ_G / G) and for rods of circular section; such equations allow to derive the uncertainties to be associated to the obtained moduli, from the intrinsic uncertainties of the primary quantities. It was estimated (ASTM, 2008) that the major sources of uncertainty come from the fundamental frequency f and from the smallest specimen dimension (thickness or diameter). Uncertainties of the moduli in the 1% range are achievable.

Other free standing sample geometries were considered, and analyzed by detailed finite elements computations, to identify the appropriate values of the numerical factor N (see Eq. (7)). Nieves et al. (2000) consider a cylinder with length equal to diameter ($L = D$). They excite vibrations by a longitudinal percussion, and detect the displacement by an optical technique; several modes are typically observed. Alfano & Pagnotta (2006) consider instead a thin square plate, and, analyzing the displacement distributions of the first modes, they identify the best positions for the plate supports and for perpendicular percussion. They measure the response by a microphone. D'Evelyn & Taniguchi (1999) similarly exploited

thin disks, exciting different modes by different impact points of a hollow zirconia bead, and measuring the response by a microphone. They exploit computations of the resonant frequencies of thin disks performed by others, and they estimate the accuracies of these computations to 1 % or better.

In all these cases, from the numerical computations the mode frequencies are tabulated or interpolated; Nieves et al. exploit the scaling parameter $\sqrt{G/\rho}/(\pi L)$. The ratios of the mode frequencies depend essentially on Poisson's ratio: the ratios of the observed frequencies allow therefore to identify the modes and to evaluate Poisson's ratio. The frequency values allow then, by the scaling parameter, to derive the shear modulus.

Both Nieves et al. and Alfano & Pagnotta perform detailed analyses of the measurement uncertainties. They both find that, also with their experimental set-up, the frequency measurement has a crucial role in the precision of the obtained moduli. Since Alfano & Pagnotta consider thin plates, they find that the precision of the thickness t is also crucial, simply because, thickness t being much smaller than the plate size a, a small value of the relative uncertainty σ_t / t is more difficultly achievable than for σ_a / a.

For comparison purposes, Nieves et al. (2000), beside considering the axial modes, also excite, by tangential percussion, the torsional modes, whose frequencies can be computed in closed form. Once the torsional modes are discriminated from the bending modes, the results agree to better than 1%, indicating a precision of this order. They also perform measurements by the pulse-echo method, finding instead discrepancies of 2% or more; they suggest that this method, which measures the propagation velocity of travelling waves, might become intrinsically less accurate when performed in a confined geometry of small size.

4.2 Resonance ultrasound spectroscopy

The Resonance Ultrasound Spectroscopy (RUS) methods have been developed (Migliori et al., 1993; Ohno, 1976; Schwarz et al., 2005; So et al., 2003) aiming in particular at the measurement of the properties of supported thin films. A recent implementation (Nakamura et al., 2004, 2010) exploits, as film support, a thin plate which, to be measured, is located on a tripod. One of the three legs is rigid, and contains a thermocouple which monitors the sample temperature; the second leg is a piezoelectric actuator, feeding a harmonic excitation whose frequency is swept, the third one is a piezoelectric sensor, which detects the oscillation amplitude. The resonance spectrum, i.e. the oscillation amplitude as function of the frequency, is measured sweeping the excitation frequency. Several peaks are found, sometimes with partial overlaps; their amplitudes, but not their frequencies, depend on the position of the piezoelectric sensor. The measurement is precise enough to clearly detect the difference between measurements in air and in vacuum, and the reproducibility of the resonance frequencies is at the 0.1 % level (Nakamura et al., 2010). The elastic constants are found fitting the computed frequencies to the measured ones; to this end, mode identification is crucial. Identification is performed keeping the excitation frequency at resonance, and scanning the specimen surface by a laser-Doppler interferometer. The map of the out-of-plane displacement of the vibrating specimen is thus obtained, which allows an unambiguous mode identification.

The elastic constants of the substrate are previously found by performing the same type of measurement on a bare substrate, and the elastic constants of the film are derived from the measured modifications of the resonance spectrum of the substrate. Since the vibration amplitude of the standing waves in a plate is maximum at the surface, the sensitivity of the

method is better than the ratio of film thickness to the support thickness. In particular, the sensitivity of each resonance frequency to each elastic constant is assessed evaluating numerically the derivatives $\partial f / \partial C_{ij}$, and from these values the uncertainties ΔC_{ij} are derived from the estimated uncertainties Δf as

$$\Delta C_{ij} = \frac{1}{\partial f / \partial C_{ij}} \Delta f \quad . \tag{11}$$

Deposited thin films often have a significant texture, with one crystalline direction preferentially oriented perpendicularly to the substrate surface, and random in-plane orientations, resulting, at a scale larger than that of the single crystallite, in in-plane isotropy, with different out-of-plane properties. This type of symmetry corresponds to the hexagonal symmetry, in which the tensor of the elastic constants is determined by five independent quantities. Among these, the resonance frequencies turn out to be almost insensitive to C_{44}, which therefore remains not determined, while the highest sensitivity is to C_{11} (Nakamura et al., 2010).

5. Laser pulse excitation

A laser pulse which is absorbed induces a sudden local heating which, by thermal expansion, produces an impulsive mechanical loading. Such a mechanical impulse excites waves in a broad frequency range, which are then detected. The accessible frequency band can be limited by either the excitation bandwidth or the detection device. According to the nature of the material being investigated, the deposition of an interaction layer can be needed. In particular, a short absorption depth is required, in order to excite a pulse which has small spatial and temporal duration, and therefore a broad band. The power density threshold for ablation must also be considered: measurements are typically conducted with high repetition rate pulses, and if ablation occurs the specimen undergoes a continuous modification during the measurement.

Two main configurations have been developed up to maturity; they differ for the propagation geometry and for the technique to detect vibrations. They are respectively called laser ultrasonics and picoseconds ultrasonics.

5.1 Laser ultrasonics

The so called laser ultrasonics technique is mainly exploited to characterize thin supported films. Oscillations are excited by a focused laser pulse, and propagation along the surface is detected, measuring the surface displacement at a distance from excitation pulse ranging from millimetres to centimetres. It is mainly the Rayleigh wave, modified by the presence of the film, which is excited and detected. The laser pulse, typically of nanosecond duration, is focused by a cylindrical lens on a line. The sudden expansion of this line source launches surface waves of limited divergence, propagating along the surface, perpendicularly to the focusing line. The component of the surface displacement normal to the surface itself can be measured, at various distances from the line source, by optical interferometry (Neubrand & Hess, 1992; Withfield et al., 2000), or, in a simpler and more robust way, by a piezoelectric sensor (Lehmann et al., 2002; Schneider et al., 1997, 1998, 2000).

The recorded displacement is frequency analyzed, yielding the dispersion relation $v(f)$ for a frequency interval that can extend over a full frequency decade (e.g. 20 to 200 MHz).

Fitting the computed dispersion relation to the measured one allows to derive the film properties. The width of the measured frequency interval can allow to to derive the Young modulus and also the film thickness (Schneider et al., 1997, 2000). The uncertainties of the results is evaluated numerically by the fitting procedure. Since the observed propagation distance is of the order of millimetres, the obtained properties are representative of an average over the propagation distance. The performance of the method could be pushed to the measurement of the properties of diamond-like carbon films having thickness down to 5 nm (Schneider et al., 2000). By stretching the observed propagation path to 20 mm it was possible to reduce the uncertainty of the measured propagation velocity of the Rayleigh wave to below 0.25 m/s. It was thus possible to detect the small variation of the Rayleigh velocity (5081 m/s for the bare (001) silicon substrate) induced by the presence of the film.
In a different configuration, the laser pulse is focused on a point instead of a line, with consequent excitation of waves which expand in all the radial directions, and a common path interferometer is adopted, whose light collection point scans the specimen surface (Sugawara et al., 2002). It is thus possible to visualize the wavefronts, circular for isotropic samples and non circular for anisotropic ones, with time resolution of the order of picoseconds and spatial resolution of a few micrometres.

5.2 Picosecond ultrasonics

The so called picosecond ultrasonics technique owes its name to the picosecond laser pulses which were available at the time it was introduced (Thomsen et al., 1984, 1986). It is nowadays implemented by femtosecond laser pulses, and is intrinsically suited to characterize thin supported films and multilayers. It follows the optical pump-and-probe scheme (Belliard et al., 2009; Bienville et al., 2006; Bryner et al. 2006; Vollmann et al. 2002). The pump beam, a femtosecond laser pulse, is focused, by a spherical lens, at the specimen surface and, at least partially, absorbed. The focusing spot, a few to tens of micrometers wide, is orders of magnitude larger than the characteristic lengths of the involved phenomena: mainly the optical absorption length, and also the thermal diffusion length and the acoustic wave propagation length, both for a femtosecond time scale. Bryner et al. (2006) estimate that with an aluminium surface, a near infrared laser (800 nm), and a pulse width of 70 fs, the absorption depth and therefore the dominant acoustic wavelength are of the order of 10 nm. Quite consistently, for a similar laser pulse but for Pt and Fe ultra thin films, Ogi et al. (2007) estimate at several THz the upper bound of the frequencies excited by the laser pulse.
The thermal and mechanical fields are thus (almost perfectly) laterally uniform, and essentially one dimensional: the absorbed pulse has a depth of the order of nanometres, and propagates like an acoustic wave with a plane wavefront which travels perpendicular to the surface, towards the specimen depth. At each interface this wave is partly transmitted and partly reflected, according to the acoustical impedances of the layers, and gives rise to echoes, which return to the surface, where they again are reflected back.
The surface is then probed by the probe beam, much weaker than the pump beam, which reaches the surface with a variable delay, controlled by a delay line. The probe beam, similarly to the acoustic wave, is partly transmitted and partly reflected at each interface, leading, in each layer, to a forward and a backward electromagnetic field, whose complex amplitudes can be calculated using a transfer-matrix formalism. The external reflectivity of the surface is the ratio of the backward to the forward complex amplitudes in the outer

space. This reflectivity is modified by the acoustic strain, by two mechanisms. Firstly, each interface is displaced by the acoustic wave, and, secondly, the refractive index in each layer is modified by the elastic strain, by the acousto-optic (also called photoelastic) coupling. In particular, it must be remembered that the traveling acoustic pulse extends over a depth of a few nanometers, inducing a localized perturbation of the refractive index, which partially scatters the optical beam. Interference can occur between the beam reflected at the outer surface and that reflected by the traveling acoustic pulse.

Interferometric techniques allow to measure the variation of both amplitude and phase of the reflected beam, thus measuring the variation of the complex reflection coefficient. With probe pulses in the femtosecond range, and varying the probe pulse delay, the time evolution of the surface reflectivity can be monitored with high temporal resolution. This time evolution typically shows several features. The diffusion, towards the sample depth, of the heat deposited by the laser pulse gives a slowly varying reflectivity background. The echoes of the acoustic pulse which, after partial reflection at the film/substrate interface, are again reflected at the outer surface are generally visible. The so called Brillouin oscillations, due to the interference between the beam reflected at the outer surface and that reflected by the traveling acoustic pulse, can then be found.

The analysis of the various features allows to characterize the waves which cross the layers travelling perpendicularly to the surface. In the derivation of the film properties, the knowledge of film thickness, typically obtained by X-ray reflectivity, has a crucial role; the uncertainty about thickness is one of the leading terms in the uncertainty of the final results. The achievable resolution depends on the excited wavelength. In copper the absorption depth is larger than the value cited above for aluminium. Since the smallness of the absorption depth determines the localization of the acoustic pulse and the achievable resolution, the deposition of an aluminium interaction layer, which guarantees a very small absorption depth, is a common practice. The interaction layer, typically a few tens of nanometres thick, then participates to the vibrational behaviour of the structure being investigated. Accurate measurements of stiffness therefore require consideration of the effects of the interaction layer, e.g. by measurements with layers of different thicknesses, followed by an extrapolation to null thickness (Mante et al., 2008). Obviously this deconvolution of the effects of the interaction layer contributes to the uncertainty of the final results.

Near infrared lasers are a common choice, because at shorter wavelength more complex phenomena can occur, which were attributed to electronic interband transitions (Devos & Cote, 2004); obviously, if one is interested in elastic properties, electronic transitions are a spurious effect to be avoided.

By picoseconds ultrasonics it was possible to characterize a layer stack, including a buried layer of about 20 nm thickness (Bryner et al., 2006). The uncertainty for the elastic constants of this layer is estimated at 20-25%, which is however remarkable for a layer of this type. The lowest limit for layer detection is also estimated at about 10 nm thickness. In a different configuration, namely a single Pt or Fe layer on a silicon substrate or a borosilicate glass substrate, Ogi et al. (2007) were able to characterize metallic films of thickness down to 5 nm. They found, at nanometric thicknesses, a dependence of the elastic moduli on thickness. This was explained by the impossibility of plastic flow at such low thicknesses: the elastic strains can thus reach levels which are non reachable in thicker samples, such that higher order elastic constants are no longer negligible.

Periodic Mo/Si multilayers (superlattices) were investigated by Belliard et al. (2009), exploring various periodicities in the nanometric range. They detect bulk waves crossing

back and forth the multilayer; such waves show pulses of the order of 10 ps, which correspond to propagation lengths much larger than the superlattice period. These waves therefore see the whole multilayer as an effective medium. The theoretical prediction for the properties of the effective medium and the reflection coefficient at the superlattice / Si substrate interface are confirmed by the experimental findings. They also detect higher frequency oscillations, which correspond to localized waves. The periodic multilayer acts as a Bragg reflector, and opens forbidden gaps in the spectrum. It can confine a mode in the neighbourhood of the outer surface (acoustic-phonon surface modes), but only if the outer layer is the lower acoustic impedance layer (in this case Si), which therefore acts as a perfect reflector. The properties of such modes could be correctly predicted only taking into account the nanometric top silicon oxide layer, which spontaneously forms at he silicon surface. The presence of this additional layer is also consistent with the X-ray reflectivity measurements. The behaviour of a Mo cavity sandwiched between Mo/Si mirrors was also analyzed.

The picoseconds ultrasonics technique was also exploited to investigate non laterally homogeneous specimens (Bienville et al., 2006; Mante et al., 2008). One limitation of this technique in the measurement of the elastic constants is that it involves only plane waves travelling perpendicular to the surface, thus allowing only the out-of-plane elastic characterization of the film. To overcome this limitation, Mante et al. and Robillard et al. (2008) proposed a technique by which the film to be characterized, and the aluminium interaction layer deposited on it, are cut by lithographic techniques to obtain a periodic square lattice of square (200 nm × 200 nm) pillars. As confirmed by the measurements performed on square lattices of different lattice constants, the pump pulse also excites, in this nanostructured film, acoustic collective modes of the pillars, which propagate along the surface in various directions. Various branches are measured, from which also the in–plane properties of the film can be measured, achieving a complete elastic characterization.

6. Brillouin spectroscopy

Aggregates of atoms, from molecules to clusters, to nanoparticles and nanocrystals, up to mesoscopic and macroscopic aggregates, can interact with electromagnetic waves either elastically or inelastically. Inelastic interactions include emission/absorption phenomena, and inelastic scattering. We consider here inelastic scattering by vibrational excitations. At the molecular scale the atomic structure of matter has a crucial role, and quantum phenomena are relevant. At this level, vibrational excitations are the vibrations of molecules, or, in a crystal, the vibrations of the internal degrees of freedom of each unit cell, which form the so called optical branches of the dispersion relation, or optical phonons. Broadly speaking, inelastic scattering by these excitations is called Raman scattering.

Aggregates above the nanometric scale also support collective vibrational excitations which begin to resemble to acoustic waves, and can be described by a continuum model. In a crystal, the vibrations of the degrees of freedom of the centre of mass of each unit cell form the so called acoustic branches of the dispersion relation, or acoustic phonons. In the long wavelength limit they are the are acoustic waves, accurately described by the continuum model (Eq. (1)). Broadly speaking, inelastic scattering by these excitations is called Brillouin scattering.

Visible light has sub micrometric wavelength. In media, either crystalline or amorphous, which are homogeneous, and therefore translationally invariant, over at least a few micrometres, vibrational excitations of sub-micrometric wavelength have a well defined

wavevector (see Eq. (2)). Due to translational invariance, the kinematics of scattering selects the excitations whose wavevector is close to the Brillouin zone center ($\mathbf{k}$ = 0). The acoustic and optical phonon branches have very different behaviours close to the zone center ($\mathbf{k} \rightarrow$ 0). The acoustic branch frequency ω_a goes to zero, with phase velocity ω_a/k and group velocity $\partial\omega_a / \partial k$ which tend to coincide with the sound velocity (which depends on polarization and, in an anisotropic crystal, on the wavevector direction), while the optical branch frequency ω_o typically goes to a maximum, with group velocity $\partial\omega_o / \partial k$ which goes to zero.

Correspondingly, with visible light and with typical properties of solids, the two types of branches produce inelastic scattering with frequency shifts ranging from a fraction of cm^{-1} to a few cm^{-1} (i.e from a few GHz to tens of GHz) for Brillouin scattering, and from hundreds to thousands of cm^{-1} (i.e from THz to tens of THz) for Raman scattering. The spectral analysis of so widely different frequency ranges requires different types of spectrometer. However, for both types of scattering the experiments are performed without exciting the vibrations, but relying on the naturally occurring thermal motion.

Brillouin spectrometry thus offers a fully optical, and therefore contact-less, method to measure the dispersion relations of bulk and surface acoustic waves, whose wavelength is determined by the scattering geometry and the optical wavelength, and is typically sub-micrometric. The frequency results from the medium properties, and typically falls in the GHz to tens of GHz range. Measurements are performed illuminating the sample by a focused laser beam, and analyzing the spectrum of scattered light, which is dominated by the elastically scattered light, but also contains weak Stokes/anti-Stokes doublets due to inelastic scattering by thermally excited vibrations (Beghi et al., 2004; Comins, 2001; Every, 2002; Grimsditch, 2001; Sandercock, 1982).

In sufficiently transparent materials scattering can occur in the bulk, by bulk acoustic waves. The coupling mechanism is the elasto-optic (or acousto-optic) effect: the periodic modulation of the refractive index by the periodic strain of the acoustic wave. In both transparent and opaque materials scattering can also occur by surface acoustic waves, by the ripple mechanism: the periodic corrugation of the surface due to the surface wave.

In more detail: the incident beam, of angular frequency Ω_i and wavelength λ_0, impinges on a sufficiently transparent sample with wavevector $\mathbf{q}_i$ and is refracted into the wavevector $\mathbf{q}'_i$. Scattered light, of wavevector $\mathbf{q}'_s$, emerges with wavevector $\mathbf{q}_s$. The probed wavevector, $\mathbf{k} = \pm(\mathbf{q}'_s - \mathbf{q}'_i)$, is determined by λ_0, the directions of $\mathbf{q}_i$ and $\mathbf{q}_s$, and the refractive index n. Light inelastically scattered by a vibrational excitation of angular frequency $\omega(\mathbf{k})$ gives a Stokes/anti-Stokes doublet at frequencies $\Omega_s = \Omega_i \pm \omega$. Detection, in the spectrum of scattered light, of such a doublet allows to measure $\omega = |\Omega_s - \Omega_i|$ and to derive the excitation velocity $v = \omega / |\mathbf{k}|$. In both transparent and opaque samples scattering occurring by surface waves only depends on the components of wavevectors parallel to the surface: the probed wavevector is $\mathbf{k}_{\|} = \pm(\mathbf{q}'_s - \mathbf{q}'_i)_{\|}$, and the surface wave velocity is $v = \omega / |\mathbf{k}_{\|}|$. In other words, the spontaneous thermal motion can be viewed as spatially Fourier transformed into an incoherent superposition of harmonic waves having all the possible wavevectors; the scattering geometry (the directions of wavevectors $\mathbf{q}_i$ and $\mathbf{q}_s$) selects a specific wavevector $\mathbf{k}$ or $\mathbf{k}_{\|}$ which is probed by the inelastic light scattering event.

Although also other geometries have been exploited (Beghi et al. 2011), in Brillouin spectroscopy the most frequently adopted scattering geometry is backscattering: $\mathbf{q}_s = -\mathbf{q}_i$. For bulk scattering it corresponds to $\mathbf{k} = \pm 2\mathbf{q}'_i$, such that

$$|\mathbf{k}| = 2\frac{2\pi}{\lambda_0} n \ , \tag{12}$$

which depends on the refractive index, but depends on geometry only when the sample is anisotropic, while for surface scattering it means $\mathbf{k}_{\|} = \pm 2\mathbf{q}_{i\|}$, i.e.

$$|\mathbf{k}_{\|}| = 2\frac{2\pi}{\lambda_0} \sin\theta \ , \tag{13}$$

where θ is the incidence angle (the angle between the incident beam and the surface normal). In this case the probed wavevector depends the incidence angle, but not on the refractive index, because Snell's law implies that upon refraction the optical parallel components $\mathbf{q}_{\|}$ remain unchanged.

The data analysis for Brillouin spectroscopy results is common to all the methods, like laser ultrasonics, which measure the velocity of travelling waves. In the simplest cases the velocity is a function of the elastic constants which can be given in closed form. For instance, if scattering by the longitudinal bulk wave, of velocity $v_l = \sqrt{C_{11}/\rho}$ (Eq. (6)) is detected, C_{11} is directly obtained as $C_{11} = \rho v_l^2 = \rho\omega^2 / k^2$, and its uncertainty $\sigma_{C_{11}}$ is evaluated by Eq. (8). In other cases, and namely in the case of supported films, the mode velocity can be computed as function of the elastic constants only numerically. In that case it must be remembered that the stiffness of an elastic solid is determined by as many independent parameters as are needed to completely identify the tensor of the elastic constants. In other words the stiffness is identified by a point in a multidimensional space, the dimensionality being 2 in the simplest case of the isotropic medium, and being higher for lower symmetry media.

Focusing here on the isotropic case, the stiffness can be represented, among other possible choices, by the (E,ν) couple (see Eqs. (3) and (4)). In Brillouin spectroscopy, for each mode the velocity is measured for various wavevectors k (in laser ultrasonics it is measured for various frequencies) as $v_m(k)$ with uncertainty $\sigma_{v(k)}$; since it can also be computed as $v_c(E,\nu,k)$, the stiffness, represented by the (E,ν) couple, can be determined by a standard least squares minimization procedure. The sum of squares is computed as

$$\chi^2(E,\nu) = \sum_k \left(\frac{v_c(E,\nu,k) - v_m(k)}{\sigma_{v(k)}} \right)^2 \ , \tag{14}$$

where, for each wavevector k, the sum is further extended to all the detected acoustic modes. Following standard estimation theory, the minimum of $\chi^2(E,\nu)$ identifies the most probable value $(\overline{E,\nu})$ of the (E,ν) couple, and the isolevel curves of the normalized estimator $\left(\chi^2(E,\nu) - \chi^2(\overline{E,\nu})\right) / \chi^2(\overline{E,\nu})$ identify the confidence region at any predetermined confidence level (Beghi et al., 2001, 2004, 2011; Lefeuvre et al., 1999). In some cases a well defined minimum of $\chi^2(E,\nu)$ is found, allowing a good identification of the parameters (Beghi et al., 2001; Comins et al., 2000; Zhang et al., 2001a), while in other cases a broad, valley-shaped minimum is found. In such cases a good identification of the parameters is not possible (Beghi et al., 2002; Zhang et al., 1998), although sometimes some combination of the parameters can be identified with better precision than individual

parameters (Comins et al., 2000; Zhang et al., 1998, 2001a). When several acoustic modes are measured, the larger amount of available information allows a precise and complete elastic characterization, as obtained e.g. for SiC films of micrometric thickness (Djemia et al, 2004).
In Eq. (14) each value $v_m(k)$, being obtained as ω/k, has an uncertainty $\sigma_{v(k)}$ which depends in turn on the uncertainty of the frequency of each spectral doublet, and on the precision of the incidence angle (see Eq. (13)) or of the refractive index (see Eq. (12)). It can be noted that the uncertainties of frequency and angle are of the random type, which affects precision but not accuracy, while the uncertainty of the refractive index affects accuracy but not precision (see Section 3.3). As with other techniques, also the uncertainties concerning the mass density and the layer thickness(es) affect accuracy but not precision. These uncertainties were the object of detailed investigations (Beghi et al., 2011; Stoddart et al., 1998). The effects of the uncertainties of the quantities which are directly measured ('primary uncertainties') on the values of the elastic constants which are finally obtained were evaluated. It was found that with appropriate sets of measurement uncertainties at the 1% level are reachable (Beghi et al., 2011).
As already noted, Brillouin spectroscopy measures the acoustic modes at frequencies of the order of GHz to tens of GHz, therefore at wavelengths much shorter than those corresponding to frequencies of tens to hundreds of MHz, typically observed with piezoelectric excitation and/or detection. This gives Brillouin spectroscopy an intrinsically higher sensitivity to the properties of films, or to the perturbation induced by the presence of very thin films. Brillouin spectroscopy was exploited to characterize tetrahedral amorphous carbon films of thicknesses of hundreds of nanometres (Chirita et al., 1999), tens of nanometres (Ferrari et al., 1999), down to a few nanometres (Beghi et al., 2002). It was also shown that inelastic light scattering can be sensitive to nanometric thickness differences (Lou et al., 2010). By Brillouin spectroscopy it was also possible to characterize buried layers in silicon-on-insulator structures (Ghislotti & Bottani, 1994).
On the other hand, the techniques which excite vibrations operate with oscillation amplitudes significantly larger than those measured by Brillouin spectroscopy; this allows more precise measurements of frequencies, which at least partially compensates for the lower intrinsic sensitivity due to the larger wavelengths. Combinations of techniques were also exploited: thicker tetrahedral amorphous carbon films films (3 micron) were characterized combining Brillouin spectroscopy and laser ultrasonics. A wide range of frequencies was thus accessible, allowing a detailed characterization of the elastic properties of the film (Berezina et al., 2004). A combination of Brillouin spectroscopy and picosecond ultrasonics was instead exploited to characterize superlattices formed by periodic multilayers of permalloy/alumina, with various periodicities at the nanometric scale (Rossignol et al., 2004). Picosecond ultrasonics characterizes the out-of-plane properties by waves travelling normal to the surface, while Brillouin spectroscopy characterizes the in-plane properties by waves travelling along the surface. The combination of techniques elucidated the effects of the interfaces.
Another algorithm for data analysis, different from that outlined above, has also been recently proposed (Every et al., 2010). Both algorithms refer to the types of waves most frequently measured in Brillouin spectroscopy of films or layered structures: surface acoustic wave, or pseudo surface acoustic waves, which essentially travel parallel to the surface, or however have a significant wavevector component parallel to the surface. It can also be mentioned that it was also possible, by Brillouin spectroscopy, to detect standing

acoustic waves trapped within a film, which are reflected back and forth, crossing the film perpendicularly to its surface (Zhang, 2001b).
Brillouin spectroscopy lends itself to the characterization of structures other than films or layers. In particular, single-walled carbon nanotubes were characterized, measuring Brillouin scattering by a free-standing film of pure, partially aligned, single-walled nanotubes, and analyzing the results in terms of continuum models (Bottani et al., 2003). The dependence of the measured spectra on the angle between the exchanged wavevector and the preferential direction of the tubes shows that the tube-tube interactions are weak: the tubes are vibrationally almost independent. The tubes are modelled as continuous membranes, at two different levels: at the first one the membrane is infinitely flexible, only able to transmit in-plane forces, while at the second level of approximation the tube wall is treated as also able to transmit shear forces and torques not belonging to the shell surface. In both cases scattering was essentially due to longitudinal waves travelling along the tubes. Taking into account that AFM images suggest that the tube segments contributing to scattering are not in the infinite tube length approximation, it was possible to derive the 2D Young modulus for the tube wall, achieving the first dynamic estimation of the stiffness of the tube wall. Scattering from carbon nanotubes was observed also in a different geometry, with an ordered array of tubes, clamped at one end (Polomska et al., 2007).
Due to its intrinsic contact-less nature, Brillouin spectroscopy is the natural choice for the measurement of elastic properties in conditions, like high temperature and/or high pressure, in which physical contact with the specimen is difficult, if possible at all. Brillouin spectroscopy only requires optical access, which can be obtained by an appropriate window, and even in the extreme conditions achievable in a diamond anvil cell, optical access is guaranteed by the transparency of the same diamond anvils.
Measurements were performed at high temperatures (Pang, 1997; Stoddart, 1995; Zhang et al., 2001a), as well as at low temperatures, which were crucial to single out a particular mechanism of hypersound propagation in alkali-borate glasses (Carini et al., 2008). After pioneering experiments at high pressures (Crowhurst et al., 1999; Whitfield et al., 1976,), in recent years dedicated Brillouin spectrometers were built at synchrotron facilities, allowing simultaneous performance of high resolution x-ray diffraction and Brillouin spectroscopy (and possibly other optical investigations like Raman spectroscopy, fluorescence, absorption) on specimens subjected to extreme pressures in a diamond anvil cell, with possible heating (Murakami et al., 2009; Prakapenka et al., 2010; Sinogeikin et al., 2006). This set-up, of particular interest for geophysicists since it allows to characterize the behaviour of minerals in the conditions which are found in the Earth's interior, was exploited to perform measurements on SiO_2 glass (Murakami & Bass, 2010) and other minerals, but also on polymers (Stevens et al., 2007) and liquid methane (Li et al., 2010).

7. Conclusion

The stiffness of films, characterized by the elastic constants, depends on the film microstructure, and its precise characterization is crucial when thin layers have structural functions. The interest in the measurement of the elastic constants is witnessed by the number of new techniques, or of improvements of existing techniques, being proposed.
The techniques which exploit either propagating acoustic waves or standing oscillations involve exclusively elastic strains: they therefore offer the most direct and clean access to the elastic properties, and potentially the most accurate measurements. Among the methods

based on vibrations, those which exploit, for excitation and/or detection, the contact-less and inertia-less nature of light, have an important role.
An overview of the variety of existing methods was presented here, trying to present a unified picture, and underlining the peculiarities of each of them, in particular for what concerns the experimental uncertainties. It turns out that, under appropriate conditions and experimental procedures, several techniques can achieve significant precision and accuracy.

8. References

Alfano, M. & Pagnotta, L., (2006). Measurement of the dynamic elastic properties of a thin coating, *Review of Scientific Instruments,* Vol.77, Paper No. 056107

ASTM E1875-08 (2008). *Standard Test Method for Dynamic Young's Modulus,Shear Modulus, and Poisson's Ratio by Sonic Resonance*, ASTM International, West Conshohocken, PA.

ASTM E1876-09 (2009). *Standard Test Method for Dynamic Young's Modulus, Shear Modulus, and Poisson's Ratio by Impulse Excitation of Vibration*, ASTM International, West Conshohocken, PA.

Auld, B. A. (1990). *Acoustic fields and Waves in Solids,* Robert E. Krieger Publishing Company, Malabar, Florida

Beghi, M. G., Bottani, C. E. & Pastorelli, R. (2001). High accuracy measurement of elastic constants of thin films by surface Brillouin scattering. In *Mechanical properties of structural films*, C. Muhlstein, C. & Brown, S.B. (Eds.), pp. 109-126. ASTM STP 1413, American Society for Testing and Materials, Conshohoken, PA

Beghi, M.G., Ferrari, A. C., Teo, K.B.K., Robertson, J., Bottani, C.E., Libassi, A. & Tanner, B.K. (2002). Bonding and mechanical properties of ultrathin diamond-like carbon films, *Applied Physics Letters*, Vol.81, pp. 3804-3806

Beghi, M.G., Every, A.G. & Zinin, P.V. (2004). Brillouin scattering measurement of SAW velocities for determining near-surface elastic properties, in *Ultrasonic nondestructive evaluation,* T. Kundu (Ed.), pp. 581-651, CRC Press, Boca Raton, FL. Revised edition in press (2011)

Beghi, M. G., Di Fonzo, F., Pietralunga, S., Ubaldi, C. & Bottani, C. E. (2011). Precision and accuracy in film stiffness measurement by Brillouin spectroscopy, *Review of Scientific Instruments,* Vol.102, Paper No. 053107

Belliard, L., Huynh, A., Perrin, B., Michel, A., Abadias, G. & Jaouen, C. (2009). Elastic properties and phonon generation in Mo/Si superlattices, *Physical Review B* Vol.80, Paper No. 155424

Berezina, S., Zinin, P. V., Schneider, D., Fei, D. & Rebinsky, D. A. (2004). Combining Brillouin spectroscopy and laser-SAW technique for elastic property characterization of thick DLC films, *Ultrasonics*, Vol.43, pp. 87 - 93

Bi, B., Huang, W.-S., Asmussen, J. & Bolding, B. (2002). Surface acoustic waves on nanocrystalline diamond, *Diamond and Related Materials*, Vol.11, pp. 677--680.

Bienville, T., Robillard, J.F., Belliard, L., Roch_Jeune, I, Devos, A. & Perrin, B. (2006). Individual and collective vibrational modes of nanostructures studied by picosecond ultrasonics, *Ultrasonics,* Vol.44, pp. e1289-e1294

Bottani, C.E., Li Bassi, A., Beghi, M.G., Podesta, A., Milani, P., Zakhidov, A., Baughman, R., Walters, D.A. & Smalley, R.E. (2003). Dynamic light scattering from acoustic modes in single-walled carbon nanotubes, *Physical. Review. B* , Vol.67, paper n. 155407

Bryner, J., Profunser, D.M., Vollmann, J., Mueller, E. & Dual, J. (2006). Characterization of Ta and TaN diffusion barriers beneath Cu layers using picosecond ultrasonics, *Ultrasonics,* Vol.44, pp. e1269-e1275

Carini, G., Tripodo, G. & Borjesson, L. (2008). Thermally activated relaxations and vibrational anharmonicity in alkali-borate glasses: Brillouin scattering study. *Physical Review B*, Vol.78, paper n. 024104

Chirita, M., Sooryakumar, R., Xia, H., Monteiro, O. R. & Brown, I. G. (1999). Observation of guided longitudinal acoustic modes in hard supported layers. *Physical Review B,* Vol.60, pp. 5153-5156.

Comins, J. D., Every, A. G., Stoddart, P. R., Zhang, X., Crowhurst, J. C. & Hearne, G. R. (2000). Surface Brillouin scattering of opaque solids and thin supported films. *Ultrasonics,* Vol.38, pp. 450-458.

Comins J.D. (2001). Surface Brillouin scattering, in *Handbook of Elastic Properties of Solids, Liquids, and Gases,* M. Levy, H. E. Bass and R. R. Stern & V. Keppens (Eds.), Volume I: *Dynamic Methods for Measuring the Elastic Properties of Solids,* pp. *349*-378, Academic Press, New York

Crowhurst, J.C., Hearne, G.R., Comins, J.D., Every, A.G. & Stoddart, P.R.. (1999). Surface Brillouin scattering at high pressure: Application to a thin supported gold film. *Physical Review B*, Vol.60, pp. R14990-R14993

Czaplewski, D.A., Sullivan, J.P., Friedmann, T.A. & Wendt, J.R. (2005). Temperature dependence of the mechanical properties of tetrahedrally coordinated amorphous carbon thin films, *Applied Physics Letters*, Vol.87, paper n. 161915

D'Evelyn M.P. & Taniguchi, T. (1999). Elastic properties of translucent polycrystalline cubic boron nitride as characterized by the dynamic resonance method, *Diamond and Related Materials*, Vol.8, pp. 1522-1526

Devos, A. & Côte, R. (2004). Strong oscillations detected by picoseconds ultrasonics in silicon: evidence for an electronic structure effect, *Physical Review B*, Vol.70, paper n. 125208

Djemia, P., Roussigné, Y., Dirras, G.,F. & Jackson, K.M. (2004). Elastic properties of SiC films by Brillouin light scattering, *Journal of Applied Physics,* Vol. 95, pp. 2324-2330

Every, A.G. (2001). The Elastic Properties of Solids: Static and Dynamic Principles, In: *Handbook of Elastic Properties of Solids, Liquids, and Gases,* M. Levy, H. Bass, R. Stern & V. Keppens (Eds.), Volume I: *Dynamic Methods for Measuring the Elastic Properties of Solids,* pp. 3-36, Academic Press, New York

Every, A.G. (2002). Measurement of the near surface elastic properties of solids and thin supported films, *Measurement Science and Technology*, Vol.13, pp. R21-R39

Every, A.G., Kotane, L.M. & Comins, J. D. (2010). Characteristic wave speeds in the surface Brillouin scattering measurement of elastic constants of crystals. *Physical Review B*, Vol.81, paper n. 224303

Farnell, G.W. & Adler, E.L. (1972). Elastic wave propagation in thin layers. In: *Physical Acoustics,* W.P. Mason & R.N. Thurston (Eds.), Vol. 9, pp. 35-127, Academic, New York

Ferrari, A. C., Robertson, J., Beghi, M. G., Bottani, C. E., Ferulano, R. & Pastorelli, R. (1999). Elastic constants of tetrahedral amorphous carbon films by surface Brillouin scattering, *Applied Physics Letters*, Vol.75, pp. 1893-1895.

Ghislotti, G. & Bottani, C. E. (1994). Brillouin scattering from shear horizontal surface phonons in silicon-on-insulator structures - Theory and experiment, *Physical Review B,* Vol.50, pp. 12131-12137.

Grimsditch, M., (2001). Brillouin scattering, in *Handbook of Elastic Properties of Solids, Liquids, and Gases,* M. Levy, H. E. Bass and R. R. Stern & V. Keppens (Eds.), Volume I: *Dynamic Methods for Measuring the Elastic Properties of Solids,* pp. 331-347, Academic Press, New York

Kim, J. Y., Chung, H. J., Kim, H. J., Cho, H. M., Yang, H. K. & Park, J. C. (2000). Surface acoustic wave propagation properties of nitrogenated diamond-like carbon films, *Journal of Vacuum Science and Technology A*, Vol.18, pp. 1993—1997

Kubisztal, M., Kubisztal, J., Chrobak, A., Haneczok, B., Budniok, A. & Rasek, J. (2008). Elastic properties of Ni and Ni + Mo coatings electrodeposited on stainless steel substrate, *Surface and Coatings Technology*, Vol.202, pp. 2292–2296

Kundu, T. (2004). Mechanics of elastic waves and ultrasonics non-destructive evaluation, in *Ultrasonic nondestructive evaluation,* T. Kundu (Ed.), pp. 1-142, CRC Press, Boca Raton, FL. Revised edition in press (2011)

Lefeuvre, O., Pang, W., Zinin, P., Comins, J.D., Every, A.G., Briggs, G.A.D., Zeller, B.D. & Thompson, G.E. (1999). Determination of the elastic properties of a barrier film on aluminium by Brillouin spectroscopy. *Thin Solid Films*, Vol.350, pp. 53-58.

Lehmann, G., Hess, P., Weissmantel, S., Reisse, G., Scheible, P. & Lunk, A. (2002). Young's modulus and density of nanocrystalline cubic boron nitride films determined by dispersion of surface acoustic waves, *Applied Physics A,* Vol.74, pp. 41—45

Li, M., Li, F.F., Gao, W., Ma, C.L., Huang, L.Y., Zhou, Q.A. & Cui, Q.L. (2010). Brillouin scattering study of liquid methane under high pressures and high temperatures. *Journal of Chemical Physics*, Vol.133, paper n. 044503

Lou, N., Groenen, J., Benassayag, G. & Zwick, A. (2010). Acoustics at nanoscale: Raman-Brillouin scattering from thin silicon-on-insulator layers, *Applied Physics Letters*, Vol.97, article n. 141908

Mante, P.A., Robillard, J.F. & Devos, A. (2008). Complete thin film mechanical characterization using picoseconds ultrasonics and nanostructured transducers: experimental demonstration on SiO_2, *Applied Physics Letters,* Vol.93, paper n. 071909

Migliori, A., Sarrao, J.L., Visschera, W.M., Bella, T.M., Leia, M., Fisk, Z. & Leisure, R.G. (1993). Resonant ultrasound spectroscopic techniques for measurement of the elastic moduli of solids, *Physica B*, Vol.183, pp. 1–24.

Murakami, M., Asahara, Y., Ohishi, Y., Hirao N. & Hirose, K. (2009). Development of in situ Brillouin spectroscopy at high pressure and high temperature with synchrotron radiation and infrared laser heating system: Application to the Earth's deep interior. *Physics of the Earth and Planetary Interiors,* Vol.174, pp. 282-291

Murakami, M. & Bass, J.D. (2010). Spectroscopic Evidence for Ultrahigh-Pressure Polymorphism in SiO_2 Glass. *Physical Review Letters*, Vol.104, pp. 025504.

Nakamura, N., Ogi, H. & Hirao, M. (2004). Resonance ultrasound spectroscopy with laser-Doppler interferometry for studying elastic properties of thin films, *Ultrasonics*, Vol.42, pp. 491–494

Nakamura, N., Nakashima, T., Oura, S., Ogi, H. & Hirao, M. (2010). Resonant-ultrasound spectroscopy for studying annealing effect on elastic constant of thin film, *Ultrasonics,* Vol.50, pp. 150–154

Neubrand, A. & Hess, P. (1992). Laser generation and detection of surface acoustic waves: Elastic properties of surface layers, *Journal of applied physics,* Vol.71, pp. 227-238

Nieves, F.J., Gascòn, F. & Bayòn, A. (2000). Precise and direct determination of the elastic constants of a cylinder with a length equal to its diameter, *Review of Scientific Instruments,* Vol.71, pp. 2433-2439

Ogi, H., Fujii, M., Nakamura, N., Shagawa, T. & M. Hirao, M. (2007). Resonance acoustic-phonon spectroscopy for studying elasticity of ultrathin films, *Applied Physics Letters*, Vol. 90, paper n. 191906.

Ohno, I. (1976). Free vibration of a rectangular parallelepiped crystal and its application to determination of elastic constants of orthorhombic crystal, *Journal of Physics of the Earth*, Vol.24, pp. 355–379.

Pang, W., Stoddart, P.R., Comins, J.D., Every, A.G., Pietersen, D. & Marais P.J. (1997). Elastic properties of TiN hard films at room and high temperatures using Brillouin scattering, *International Journal of Refractory Metals and Hard Materials*, Vol.15, pp. 179-185.

Polomska, A.M., Young, C.K., Andrews, G.T., Clouter, M.J., Yin, A. & Xu, J. M. (2007). Inelastic laser light scattering study of an ordered array of carbon nanotubes. *Applied Physics Letters*, Vol.90, paper n. 201918

Prakapenka, V. (2010). On-line Brillouin Spectroscopy at GSECARS: Basic Principles and Application for High Pressure Research, *Synchrotron Radiation News* Vol.23, pp. 14-15.

Robillard, J.-F., Devos, A., Roch-Jeune, I. & Mante, P. A. (2008). Collective acoustic modes in various two-dimensional crystals by ultrafast acoustics: Theory and experiment, *Physical Review B*, Vol.78, paper n. 064302

Rossignol, C., Perrin, B., Bonello, B., Djemia, P., Moch, P., & Hurdequint, H. (2004). Elastic properties of ultrathin permalloy/alumina multilayer films using picosecond ultrasonics and Brillouin light scattering, *Physical Review.B,* Vol.70, paper n. 094102

Sandercock J.R. (1982). Trends in Brillouin scattering – Studies of opaque materials, supported films, and central modes, in *Light Scattering in solids III*, M. Cardona and G. Güntherodt (Eds.), pp. 173-206, Springer, Berlin

Schneider, D., Schwarz, T., Scheibe, H.-J. & Panzner, M. (1997) Non destructive evaluation of diamond-like carbon films by laser induced surface acoustic waves, *Thin Solid Films, Vol.*295, pp. 107—116

Schneider, D., Schultrich, B., Scheibe, H.-J., Ziegele, H. & Griepentrog, M. (1998). A laser acoustic method for testing and classifying hard surface layers, *Thin Solid Films,* Vol. 332, pp. 157—163.

Schneider, D., Witke, T.H., Schwarz, T.H., Schoneich, B. & Schultrich, B. (2000). Testing ultra-thin films by laser-acoustics, Surface and Coatings Technology, Vol.126, pp.136-141

Schwarz, R.B., Hooks, D.E., Dick, J.J. & Archuleta, J.I. (2005). Resonant ultrasound spectroscopy measurement of the elastic constants of cyclotrimethylene trinitramine, *Journal of Applied Physics*, Vol.98, paper N. 056106.

Sinogeikin, S., Bass, J., Prakapenka, V., Lakshtanov, D., Shen, G.Y., Sanchez-Valle, C & Rivers, M. (2006). Brillouin spectrometer interfaced with synchrotron radiation for simultaneous X-ray density and acoustic velocity measurements. *Review of Scientific Instruments*, Vol.77, article n. 103905

So, J.H., Gladden, J.R., Hu, Y.F., Maynard, J.D. & Qi Li (2003). Measurements of elastic constants in thin films of colossal magnetoresistance material, *Physical Review Letters*, Vol.90, paper N. 036103.

Stevens, L.L., Orler, E.B., Dattelbaum, D.M., Ahart, M. & Hemley, R. J. (2007). Brillouin scattering determination of the acoustic properties and their pressure dependence for three polymeric elastomers. *Journal of Chemical Physics*, Vol.127, article n. 104905

Stoddart, P.R., Comins, J.D. & Every, A.G. (1995). Brillouin-scattering measurements of surface-acoustic-wave velocities in silicon at high-temperatures. *Physical Review B*, Vol.51, pp. 17574-17578

Stoddart, P.R., Crowhurst, J.C., Every, A.G. & Comins, J. D. (1998). Measurement precision in surface Brillouin scattering, *Journal of the Optical Society of America B*, Vol.15, pp. 2481-2489.

Sugawara, Y., Wright, O.B., Matsuda, O. & Gusev, V.E. (2002). Spatiotemporal mapping of surface acoustic waves in isotropic and anisotropic materials, *Ultrasonics,* Vol.40, pp. 55-59

Thomsen, C., Strait, J., Vardeny, Z., Maris, H.J., Tauc, J. & Hauser, J.J. (1984). Coherent phonon generation and detection by picoseconds light pulses, *Physical Review Letters*, Vol. 53, pp. 989-992

Thomsen, C., Grahn, H.T., Maris, H.J. & Tauc, J. (1986). Surface generation and detection of phonons by picoseconds light pulses, *Physical Review B*, Vol. 34, pp. 4129-4138

Vollmann, J., Profunser, D.M. & Dual, J., (2002). Sensitivity improvement of a pump-probe set-up for thin film and microstructure metrology, *Ultrasonics,* Vol.40, pp. 757–763

Whitfield, C.H., Brody, E.M. & Bassett, W.A. (1976). Elastic moduli of NaCl by Brillouin scattering at high pressure in a diamond anvil cell. *Review of Scientific Instruments*, Vol.47, pp. 942-947

Whitfield, M. D., Audic, B., Flannery, C. M., Kehoe, L. P., Crean, G. M. & Jackman, R. B. (2000). Charactrization of acoustic Lamb wave propagation in polycrystalline diamond film by laser ultrasonics, *Journal of Applied Physics,* Vol.88, pp. 2984—2993.

Zhang, X., Comins, J.D., Every, A.G. & Stoddart, P.R. (1998). Surface Brillouin scattering studies on vanadium carbide, *International Journal of Refractory Metals and Hard Materials*, Vol.16, pp. 303-308

Zhang, X., Stoddart, P.R., Comins, J.D. & Every, A. G. (2001a). High-temperature elastic properties of a nickel-based superalloy studied by surface Brillouin scattering, *Journal of Physics: Condensed. Matter*, Vol.13, pp. 2281-2294

Zhang, X., Sooryakumar, R., Every, A.G. & Manghnani, M.H. (2001b). Observation of organpipe acoustic excitations in supported thin films. Physical Review B, Vol.64, paper n. 081402.

Zinin, P.V (2001). Quantitative acoustic microscopy of solids, in *Handbook of Elastic Properties of Solids, Liquids, and Gases,* M. Levy, H. E. Bass and R. R. Stern & V. Keppens (Eds.), Volume I: *Dynamic Methods for Measuring the Elastic Properties of Solids,* pp. 187-226, Academic Press, New York

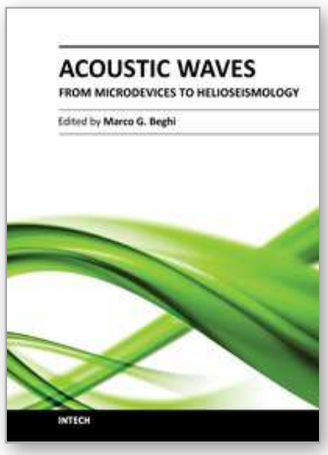

Acoustic Waves - From Microdevices to Helioseismology

Edited by Prof. Marco G. Beghi

ISBN 978-953-307-572-3
Hard cover, 652 pages
Publisher InTech
Published online 14, November, 2011
Published in print edition November, 2011

The concept of acoustic wave is a pervasive one, which emerges in any type of medium, from solids to plasmas, at length and time scales ranging from sub-micrometric layers in microdevices to seismic waves in the Sun's interior. This book presents several aspects of the active research ongoing in this field. Theoretical efforts are leading to a deeper understanding of phenomena, also in complicated environments like the solar surface boundary. Acoustic waves are a flexible probe to investigate the properties of very different systems, from thin inorganic layers to ripening cheese to biological systems. Acoustic waves are also a tool to manipulate matter, from the delicate evaporation of biomolecules to be analysed, to the phase transitions induced by intense shock waves. And a whole class of widespread microdevices, including filters and sensors, is based on the behaviour of acoustic waves propagating in thin layers. The search for better performances is driving to new materials for these devices, and to more refined tools for their analysis.

How to reference

In order to correctly reference this scholarly work, feel free to copy and paste the following:

Marco G. Beghi (2011). Acoustic Waves: A Probe for the Elastic Properties of Films, Acoustic Waves - From Microdevices to Helioseismology, Prof. Marco G. Beghi (Ed.), ISBN: 978-953-307-572-3, InTech, Available from: http://www.intechopen.com/books/acoustic-waves-from-microdevices-to-helioseismology/acoustic-waves-a-probe-for-the-elastic-properties-of-films

INTECH
open science | open minds

InTech Europe
University Campus STeP Ri
Slavka Krautzeka 83/A
51000 Rijeka, Croatia
Phone: +385 (51) 770 447
Fax: +385 (51) 686 166
www.intechopen.com

InTech China
Unit 405, Office Block, Hotel Equatorial Shanghai
No.65, Yan An Road (West), Shanghai, 200040, China
中国上海市延安西路65号上海国际贵都大饭店办公楼405单元
Phone: +86-21-62489820
Fax: +86-21-62489821

IntechOpen